STRUCTURAL AND FUNCTIONAL PECULIARITIES OF SPINE DEFORMITY DEVELOPMENT IN NEUROFIBROMATOSIS NF-1*

A.M. Zaidman, M.V. Mikhailovsky, T.N. Sadovaya
Novosibirsk Research Institute of Traumatology and Orthopedics

Objective. To study pathogenetic mechanisms of the development of spinal deformity in neurofibromatosis.
Material and Methods. Structural components of the spine were presented as specimens obtained after surgical correction of spinal deformity performed in 10 children with grade III—IV scoliosis associated with neurofibromatosis. Tissues were investigated by conventional histochemical and ultrastructural methods. The levels of aggrecan and lumnican gene expression were studied using PCR method.
Results. Etiologic factor of the development of spinal deformity in neurofibromatosis is a mutation of the NF-1 gene in cells of ganglious lamella. Migration of cells carrying mutant gene into one of the sclerotome zones results in oncogene activation and intensive proliferation of chondro-, osteo-, and fibroblasts in the growth plate, intervertebral disc, and vertebral body. Since the mutation involves the earliest stages of embryogenesis, the formation of definitive structural components in pathologically altered zones is disturbed.
Conclusion. Progressive development of the spinal deformity after surgical intervention is accounted both for proliferation of chondro- and fibroblasts in the vertebral body and intervertebral disc and for disturbance of the lumnican gene expression.
Key Words: neurofibromatosis, growth plate, sclerotome, spinal deformity, gene expression.

** Zaidman A.M., Mikhailovsky M.V., Sadovaya T.N. [Structural and Functional Peculiarities of Spine Deformity Development in Neurofibromatosis NF-1]. Hirurgia pozvonocnika. 2008;(3):73–80. In Russian. DOI: https://doi.org/10.14531/ss2008.3.73-80*

Neurofibromatosis type I is a severe systemic disease that mostly affects skin, as well as the nervous, muscular, and skeletal systems. It is an autosomal-dominant hereditary disease with high penetrance and variable expressivity of the genotype [15]. The etiologic factor of the disease is mutation in the NF-1 gene located on chromosome 17q [15, 19].

The NF-1 mutation increases activity of Ras oncoproteins, thus leading to cell proliferation and tumor development. Spine deformities, thoracic kyphosis and scoliosis, are the most common (2–69 %) bone lesions associated with neurofibrosis [4–8, 10, 11, 15, 17, 18]. The mechanism of a spine deformity remains unknown. According to A.J. Tsirilios et al. [20], a spine deformity is a result of tumor (neurofibrome) pressure on vertebral bodies [8–10].

Primary mesoderm dysplasia, osteomalation, and endocrine imbalance are other candidate underlying diseases [14, 16]. Nevertheless, none of these theories have been reliably proven. Idiopathic neurofibromatosis, sharing the clinical and radiographic details with idiopathic scoliosis, is the hardest-to-explain neurofibromatosis type that can only be diagnosed by the concomitant symptoms [10, 12, 13, 16].

No data on morphological changes in spine structural components in patients with neurofibromatosis are available from the existing literature. For this reason, the pathogenic mechanisms of the development of spine deformities in patients with neurofibromatosis were examined in this study.

Material and Methods

Growth plates (GP), intervertebral discs, and vertebral bodies used in this study were obtained from ten 10 to 14-year-old patients with grade III-IV scoliosis associated with neurofibromatosis at the Clinic of Children Vertebrology, Novosibirsk Research Institute of Traumatology and Orthopaedics. Structural components of spines of 12 to 14-year-old children obtained at the Chair of Forensic Medicine were used as controls.

Tissues were fixed in 10 % formalin solution; bone tissue was decalcified in cold versene. Deparafined sections were stained histologically (Van Gieson hematoxylin-eosin and Mallori) or histochemically (toluidine blue at various pH, Alcian Blue and Hale-, PAS (periodic-acid-Schiff)-, and Green reactions).

Material for ultrastructural studies was first fixed in 4 % paraform solution, then in 1 % OsO solution, dehydrated in progressively more concentrated ethanol, and embedded into Epon-Araldite. Ultrathin sections were prepared using a microtome, contrasted with uranyl acetate, and viewed under an electron microscope.

Cells isolated from GPs of vertebral bodies of IS patients (surgical material) served as source material in the study of the expression level of candidate

genes. The chondroblasts isolated from GPs of vertebral bodies of 12–14-year-old children were used as controls. The hyaline cartilages were washed in Hanks' solution containing 1 g/L kanamycin for 15 min, cut in a Petri dish with the minimal volume of RPMI medium into 1–2 mm^2 slices, placed into 1.5 % collagenase solution in a siliconized dish, and shaken for 5–8 h at 37 °C. The resulting suspension was filtered through nylon and centrifuged at 1,500 rpm for 10 min.

Primers for human aggrecan (NM013227, GI: 6995993), and lumnican (NM 002345, GI: 21359858) genes were used for polymerase chain reaction (PCR).

i-RNA was isolated from chondrocytes of both IS patients and controls using a TRIzol kit.

RNA was purified from DNA by adding DNAse (1 AU) to 40 µL of isolated RNA solution. The solution was adjusted up to 100 µL with an appropriate buffer, and incubated at 37 °C for 30 min. 100 µL of phenol was added to the solution and stirred. After 40 µL of chloroform was added, the mixture was centrifuged at 7,500 rpm for 5 min. The water phase was transferred to a clean tube, supplemented with 100 µL of isopropanol, incubated at room temperature, and centrifuged at 12,000 rpm for 10 min. The resulting precipitate was washed with 200 µL of 75% ethanol and centrifuged at 7,500 rpm for 5 min. The washed precipitate was dried, dissolved in 40 µL of water, and incubated at 55 °C for 10 min.

For reverse transcription, 10 pmole of primers (OligodT or random hexanucleotide primers) was added to 2 µg of isolated RNA, incubated at 70 °C for 5 min, cooled with ice for 1 min, and shaken. Further, 5 µL of buffer for reverse transcription, 0.5 mmole of each desoxynucleoside triphosphate, and 200 AU of M-MTLV reverse transcriptase were added in a strict order; the solution volume was adjusted to 25 µL with water and incubated at 37 °C for 1 h.

The fragments of the lumnican, aggrecan, and GAPHD genes were amplified using the multiplex PCR at a Tertsik amplifier using the GAPHD gene as a control. 20 µL of the reaction mixture contained approximately 200 ng of cDNA, 2 µL of 10x PCR buffer (10 mM Tris-HCl, 1.5 mM MgCl, and 50 mM KCl, pH 8.3), 20 pmole of each primer, 0.2 mmole of each desoxynucleoside triphosphate, and one AU of Taq DNA polymerase. The reaction mixture was covered with the equal volume of a mineral oil. The PCR conditions were as follows: initial denaturation at 95 °C for 5 min, annealing of primers at 55 °C for 30 s, elongation at 72 °C for 60 s, and final elongation at 72 °C for 10 min.

The PCR products were analyzed using the horizontal gel-electrophoresis in 0.9 % agarose gel in TAE buffer (0.04 M Tris-HCl, 0.05 M EDTA pH 8.0) containing 1 µg/mL of ethidium bromide. DNA of the pBlueScript/SK plasmid processed with MspI restriction endonuclease, 100 bp, and 1 kb fragments of marker DNA were used as molecular weight standards.

The DNA solution was mixed with 50 % glycerol containing 0.1 % Bromophenol blue and 0.1 % xylene cyanole solutions at a 1:10 ratio, and placed on the gel. Electrophoresis took 20 min at 6 to 8 V/cm electric field intensity. The gels were UV-scanned using a videosystem.

Results

The clear boundary between the convex and concave sides of the deformity can be seen in the GP of vertebral bodies at the deformity level. The matrix looks like a cell-free zone of non-uniform structure and color (Fig. 1, 2). A V-shaped protrusion (invagination) limited by a thin bone plate can be seen between the medial and lateral portions of the GP (subchondral zone) at the boundary of the vertebral body (Fig. 3). The GP structure at the convex side above and below the deformity is consistent with the age norm. The chondroblasts with clear zonal differentiation can be seen

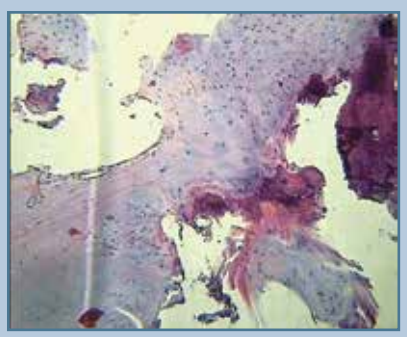

Fig. 1
Growth plate of the vertebral body; boundary between the convex and concave sides of the curvature; hematoxylin and eosin staining (10 x 20)

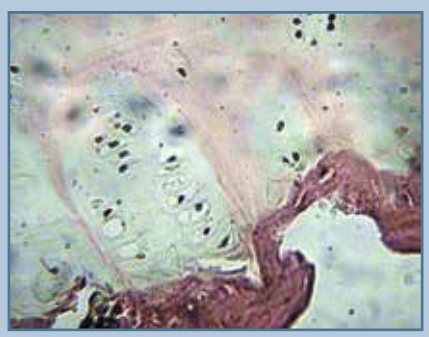

Fig. 2
Growth plate of the vertebral body at the deformity level; boundary between the convex and concave sides of the curvature; Van Gieson staining (10 x 40)

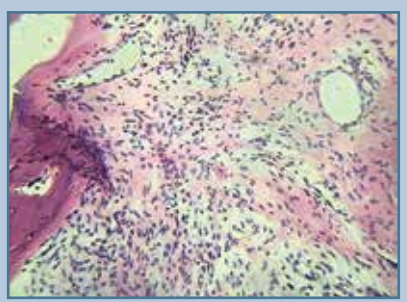

Fig. 3
Proliferation of the poorly differentiated chondroblasts in the growth plate of the vertebral body at the concave side of the curvature; hematoxylin and eosin staining (10 x 20)

against the homogenous Alcian-positive matrix. The surface layer contains isolated poorly differentiated chondroblasts with central or excentral nucleus and basophilic cytoplasm. The proliferation zone contains medium-differentiated chondroblasts with small granules of glycogen and chondroitin sulfate A and C in the cytoplasm (Fig. 4). Intense γ-metachromasia and the Hale reaction can be seen in moderately PAS-positive matrix surrounding the cell (Fig. 5). The differentiated chondrocytes with a well-defined chondron structure and the corresponding topochemical characteristics form the core layer. The chondroitin sulfates surround the lacunes. The interterritorial matrix contains both A and C chondroitin sulfates, and keratan sulfates in the area of the chondro/hematic barrier. The hypertrophic chondrocytes are localized at the boundary with subchondral bone tissue. Vascular invasion is almost non-pronounced; this fact is presumably associated with the corresponding growth phase. Thin trabeculae of vertebral bodies are atrophic, and the adhesion lines are not clear. The regular arrangement of osteocytes is disturbed, and neither the osteoblast reaction nor osteoids can be found near the trabeculae. Osteoblast cytoplasm is Hale-negative, but trace Alcian blue reaction can be seen (Fig. 6).

In some samples (grade IV scoliosis) trabeculae were severely thinned and atrophic at the deformity level (Fig. 7).

Collagen fibers of the fibrosis ring form compact fascicles with thin sheets of loose Alcian-positive pale connective tissues. The pulpous nucleus in some samples consisted of proliferates of fibro- and chondroblasts invading the intervertebral disc from the concave side of the deformity (Fig. 8a). In some samples, these proliferates formed isolated round-shaped tumor-like structures consisting of poorly differentiated chondroblasts and homogenous cartilage matrix (Fig. 8b) or fibroblasts surrounded with fibrous tissue. At the concave side, the structure of GP of a vertebral disc at the deformity level was heterogeneous. In some samples, the proliferation zones of poorly differentiated embryonic-

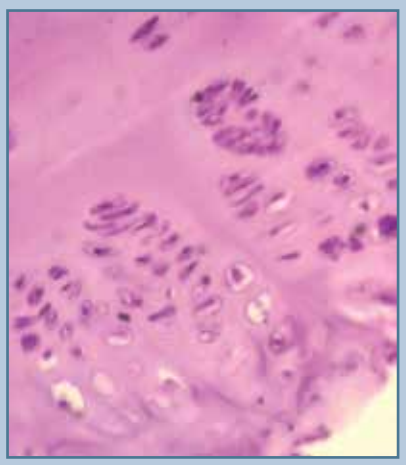

Fig. 4
Glycogen granules in cytoplasm of the growth plate cells at the concave side of the curvature; PAS-reaction (10 x 40)

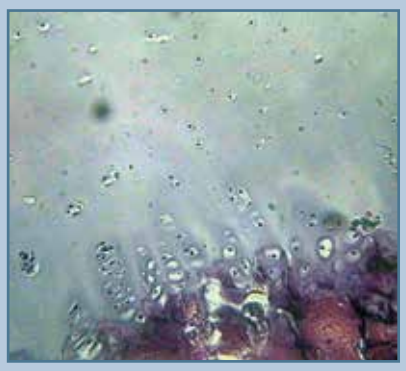

Fig. 5
Highpolymer chondroitin sulfates in chondroblasts cytoplasm and matrix at the concave side of the curvature; Hale reaction (10 x 20)

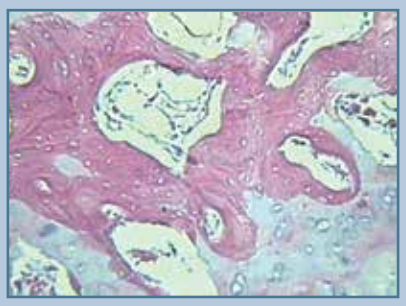

Fig. 6
Primitive trabeculae; osteogenesis is not expressed; hematoxylin and eosin staining (10 x 20)

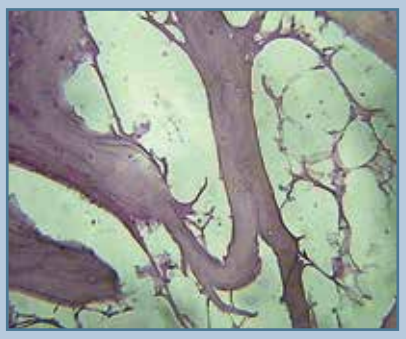

Fig. 7
Severe atrophy of the bone tissue at the concave side of the curvature (grade IV deformity); hematoxylin and eosin staining (10 x 20)

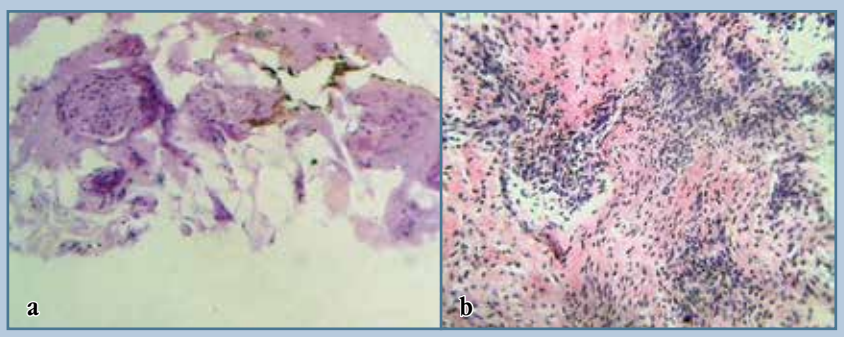

Fig. 8
Proliferation of chondroblasts in the pulpous nucleus, PAS-reaction (10 x 10) **(a)** and of chondro- and fibroblasts in the loose-fibrous part of the disc, hematoxylin and eosin staining (10 x 10) **(b)**

type chondroblasts with large nucleus and narrow cytoplasm ring can be seen against the background of homogenous chondromucoid and rare chondroblasts (Fig. 9). These cells have either radial or chaotic localization. Cystic cavities and necrotic foci can be seen in the center of cell aggregations (Fig. 10). In other samples, proliferates of chondro- and fibroblasts that are tightly adjacent to the primitive bone tissue can be seen in GP along with the described structures (Fig. 11).

No proliferates of such type can be seen in the other sites. A wavy meandering invasion of proliferating cartilage into the vertebral body can be seen against the dystrophic matrix and isolated chondroblasts with eosinophilic cytoplasm and picnotic nucleus. The proliferating tissues are bounded with thin trabeculae. This structure provides the radiological scallop pattern of vertebral bodies.

The matrix of some samples had cystic cavities of various dimensions against chondroblast proliferation, while in some other samples, fragmented round-shaped Alcian-positive sites of cartilage tissue with pronounced dystrophy of both matrix and cells can be seen (Fig. 12).

The intense Alcian-positive reaction can be seen in zones of proliferating chondroblasts and in matrix. Hyaluronidase control allowed us to identify hyaluronic acid and chondroitin sulfate C. Unmasked collagen fibers can be found in the dystrophy zones.

The boundary between the vertebral body and GP is formed by proliferating tissues composed of primitive cells that invade the vertebral body; these cells are bounded by chaotic agglomeration of trabeculae at the mineralization stage (Fig. 13). Moderate quantities of osteoclasts can be seen in Gaupshipt lacunas. Cell-free trabeculae in the vertebral body are thinned. Osteoblast reaction is absent. Cystic cavities and adipose marrow with rare fields of accumulation of myeloid cells are located among the trabeculae.

At the convex side, a pulpous nucleus is absent because of total severe fibroblast cellularity of the disc. Below and above the spine deformity level, dys-

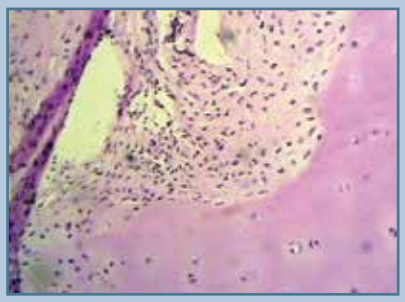

Fig. 9
Proliferation of the poorly differentiated chondroblasts in the growth plate at the concave side of the curvature, PAS-reaction (10 x 10)

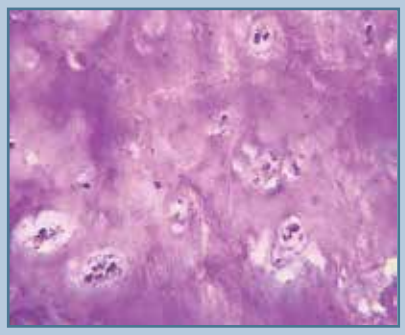

Fig. 10
Necrotic and apoptotic foci in the center of proliferates of the growth plate (the concave side of the curvature), PAS-reaction (10 x 20)

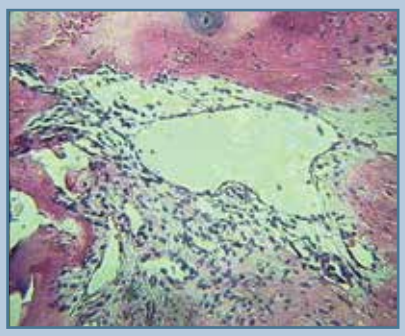

Fig. 11
Cystic cavities; proliferation of chondroblasts in the growth plate at the concave side of the curvature; scallop pattern of the vertebral body, hematoxylin and eosin staining (10 x 20)

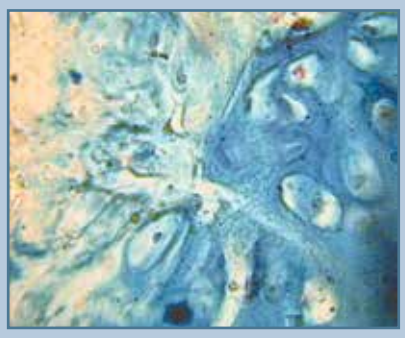

Fig. 12
Chondroitin sulfates in the chondroblast cytoplasm and matrix of the growth plate of the vertebral body; Alcian-blue staining (10 x 100)

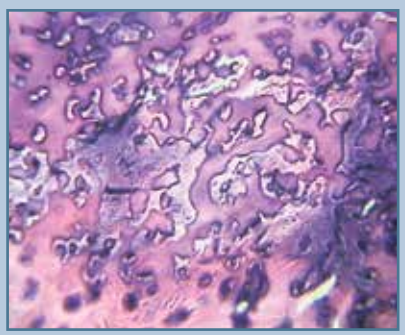

Fig. 13
Chaotic localization of trabeculae at the mineralization stage (concave side of the curvature); hematoxylin and eosin staining (10 x 10)

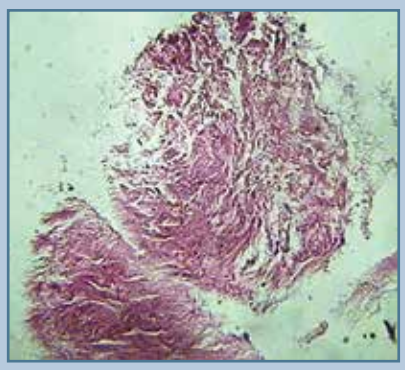

Fig. 14
Tumor-like neoplasm in the intervertebral disc; hematoxylin and eosin staining (10 x 20)

trophic changes in the disc are less pronounced; there remain thin sheets of ground substance, in which chondroitin sulfates C and hyaluronic acid can be found. Small glycogen granules can be found in cell cytoplasm. At the deformity level, cell groups represented by poorly differentiated proliferating chondroblasts and (or) fibroblasts that form tumor-like structures localize in the intervertebral disc along with its dystrophic changes (Fig. 14). In some samples, these cells form concentric and sometimes palisade structures (Fig. 15, 16). Proliferates of fibroblasts and fibrocytes adjacent to GP can be randomly seen.

In the proliferation zones, expression of the lumnican gene in GPs, discs and adjacent bone tissue (the convex side) is dramatically decreased against the pronounced expression of the aggrecan gene (Fig. 17).

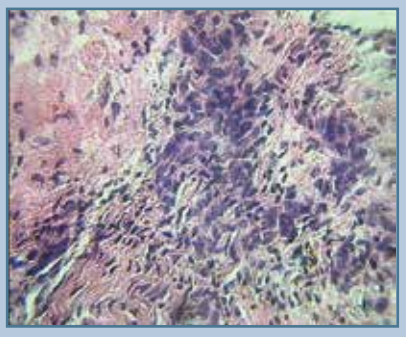

Fig. 16
Aggregation of large cells in the intervertebral disc among the collagen fibers; some cells form palisade structures; the others form vortices; mitotic division can be seen in some cells (10 x 40)

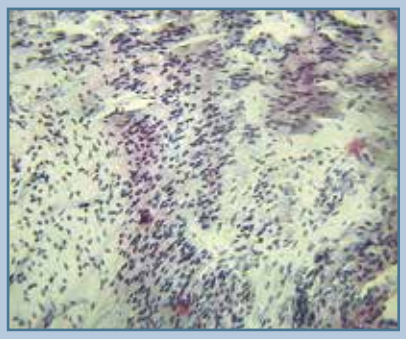

Fig. 15
Palisade structures in the intervertebral discs at the concave side; Alcian-blue staining (10 x 20)

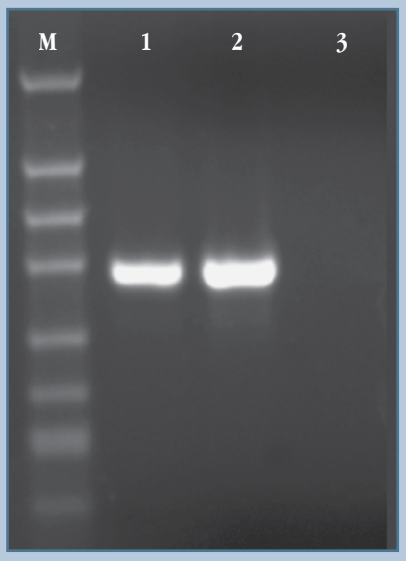

Fig. 17
PCR analysis of the aggrecan and lumnican genes: M is the molecular weight marker (product of pBluescript/SK hydrolysis by MspI restriction endonuclease); 1 – expression of the aggrecan gene in a patient with neurofibromatosis at the convex side; 2 – expression of the aggrecan gene at the concave side; 3 – disturbed lumnican gene expression in a patient with neurofibromatosis

Discussion

Morphological studies of spine structural components have demonstrated that a PR of the convex side is presented by small tightly packed and randomly oriented cells (sometimes in the dystrophic matrix). In terms of their phenotypical characters, ultrastructural organization, and morphological characteristics, these cells are poorly differentiated embryonic chondroblasts. This brings up the following questions: how can the embryo-type cells be maintained in a GP? Why does neither cell differentiation nor specialization take place? The origin of these cells and of the reason behind their active primitive proliferation should be considered to answer this question. Neurofibromatosis is known to be an autosomal dominant pathology associated with the mutation in the NF-1 gene in ganglion cells. Being derivatives of neuroectoderm, the cells of the ganglion plate settle between the ecto- and endoderm in the early gastrulation to form neural ganglia, the adrenal medulla, the vegetative nervous system, bones, cartilage formations in the facial and cranial skull, dentin, etc. (Fig. 18). It is believed that cells of the ganglion plate also migrate into the mesoderm rudiments. This idea can be confirmed by Recklinghausen disease (presence of multiple neurofibromes in the derm – a derivative of the segmented mesoderm). Moreover, proliferation of chromatophores in the epidermis is a factor for the formation of café au lait spots, one of the main neurofibromatosis symptoms. These facts attest to possible migration of the ganglion plate cells into dermatome and sclerotome, which is consistent with the classical statement of H. A. E. Driesch that while the process of cell movement is uniform, a trajectory of a single cell may be somewhat random (quoted in: LV. Belousov, 1980). In line with the main concept of embryology, migration of glial plate cells with NF-1 mutation into the sclerotome causes alterations of the glial plate phenotype. The fate of neural crest cells has not been determined thus far; hence, the migrating cells acquire the phenotype of a new environment [2].

At the stage of chondrogenic differentiation of the sclerotome, the cells of the ganglion plate look phenotypically like the embryonic chondroblasts, but their genotype (NF-1 mutation) does not disappear. NF-1 is a tumor-suppressor gene expressing neurofibromin. This gene

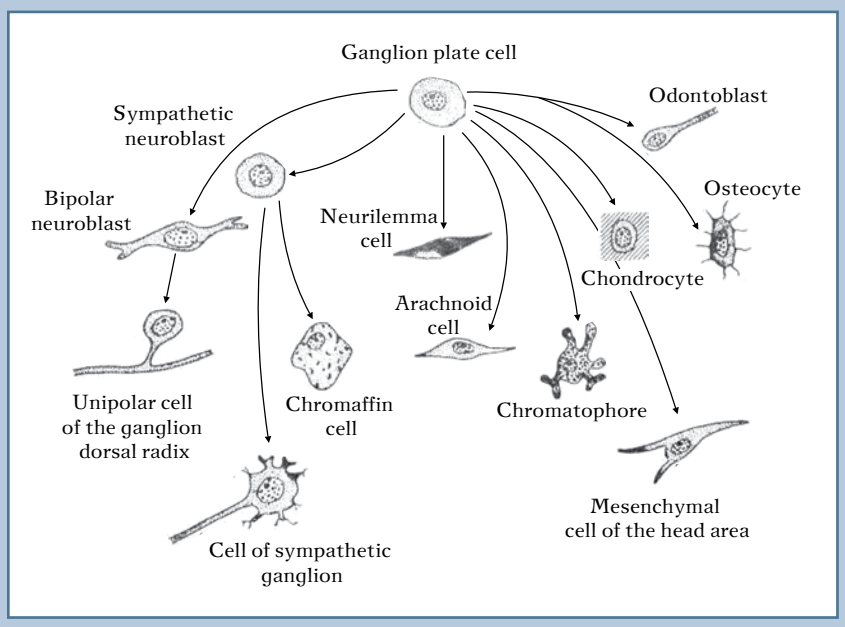

Fig. 18
Fate of the growth plate cells according to A.G. Knorre [2]

controls activity of the Ras family oncoproteins by converting these proteins to the GDF-bound forms. Mutations in one of the NF-1 alleles cause increased activity of Ras oncoproteins leading, thus, to active cell division and tumor formation. In the GPs they are presented by chaotic, sometimes radial, poorly differentiated chondroblasts with the embryonic competence. These cells lack specialized structures or specific functions; they have general purpose organelles inherent in any cell and perform general functions only; i.e. nutrition, respiration, secretion, movement, growth, and reproduction [2]. In early morphogenesis, a great deal of cells ensure the formation of the matrix and tissue-specific structures by synthesis aimed at forming tissue-specific organelles and receptor complex of the cells.

The auto-paracrine regulation is followed by an appropriate hierarchical regulation, when inter-tissue interactions ensuring homeostasis of the functioning organ occur. Tissue specificity of a cell is a stage preceding its organ specificity.

Disorder in the development of organ specificity of GP chondroblasts at the convex side causes growth asymmetry. Primitive chondroblasts do not undergo stages of differentiation; that is, they neither integrate into chondrons nor form specific receptors capable of perceiving regulative signals of the hormonal and other systems. Isolated cells do not perceive induction and are incapable of synthesizing specific enzymes [3]. NF-1 mutations break the obligatory sequence of the form-building process: cell — tissue — organ. Disorders in specific proliferation and chondroblast differentiation processes are followed by dramatic change in osteogenesis. Chaotic formation of demineralized trabeculae, similar to that in the GP, can be seen against the proliferation of osteoblasts and osteoclasts.

Intense proliferation of GP chondroblasts continues beyond its boundaries. The proliferates invade the vertebral body, thin bone plates become their boundaries, determining the scallop pattern of the vertebral body, which is one of the radiological symptoms of the pathology under consideration.

Derangement of the bone tissue structure is associated with the activity of Ras-proteins stimulating the mitotic activity of osteoblasts against low expressiveness of the lumnican gene (Fig. 17). These genes regulate different stages of ontogenesis; therefore, their dual impact cannot be excluded.

Alterations in the intervertebral disc are of a particular interest. Both isolated proliferates consisting of poorly differentiated chondroblasts and neurofibrome-like formations can be seen at various disc sections at the convex side of the deformity. Palisade structures can be found in some samples. These facts prove the concept that the phenotype of the ganglion plate depends on a migration site.

The process of spine deformity formation associated with neurofibromatosis is one of the main problems. Morphological studies attest to the derangement of structural organization of GP at the convex side of the deformity, while the regularities and stage patterns of chondroblast differentiation and adequate osteogenesis remain unchanged at the concave side. Regularities of independent development of different parts of the vertebral bodies and differentiated gene regulation of these areas confirm the idea that ganglion plate cells may migrate to one of the rudiments of the structural components of the spine being formed. The presence of a clear boundary between the convex and concave sides of the curvature is also indicative of this fact. The continued growth (adequate proliferation, differentiation and osteogenesis at the convex side of the curvature and severe disturbance of the growth function at the concave side of the curvature) is the reason for growth asymmetry and spine deformity formation. Spine deformities in patients with both neurofibromatosis and idiopathic scoliosis result from genetic growth disorders; nevertheless, these pathologies have different pathogenetic mechanisms.

Deformity progression after a surgical intervention is one of the typical features of scoliosis associated with neurofibromatosis. Deformities progression (modulation) should be considered in connection with continued proliferative activity in the spine structural components: intervertebral disc, vertebral body,

and cartilage tissue. In patients with the pathology under study, the pathological process involves all spine structural components and not only GP as it is in case of idiopathic scoliosis.

Cell proliferation in the vertebral body should be considered as the blastomatose process. In such a case, both the progression of the spine deformity (modulation) and false joints formed after a surgical intervention can be explained as the continued proliferation of the chondro- and fibroblasts in the intervertebral disc and disturbed lumnican gene expression.

Conclusion

NF-1 mutation in ganglion plate cells is an etiological factor of spine deformity formation in patients with neurofibromatosis. Migration of cells carrying the mutant gene into of the sclerotome zones causes tumor gene proliferation and intense proliferation of chondro-, osteo-, and fibroblasts in the GP, intervertebral disc, and vertebral body. This mutation involves the earliest embryogenesis, formation of definitive structural spine components (in particular, the growth organ); therefore, the growth process in pathologically altered zones is impaired. The continued spine deformation (modulation) after a surgical intervention can be explained by both proliferation of chondron- and fibroblasts in the vertebral body and intervertebral disc and impairment of the lumnican gene expression.

References

1. **Belousov LV.** [Introduction to General Embryology]. Moscow, 1980. In Russian.
2. **Knorre AG.** [Embryonic Histogenesis]. Leningrad, 1971. In Russian.
3. **Korochkin LI.** [Gene Interaction during Development]. Moscow, 1977. In Russian.
4. **Biesecker LG.** [The multifaceted challenges of Proteus syndrome]. JAMA. 2001; (285): 2240–2243.
5. **Buniatov RN.** [Clinical X-ray characteristics of scoliosis in neurofibromatosis]. Pediatriya. 1983; (5): 49–51. In Russian.
6. **Calvert PT, Edgar MA, Webb PJ.** [Scoliosis in neurofibromatosis. Natural history with and without operation]. J. Bone Joint Surg. Br. 1989; (71): 246–251.
7. **Cawthon RM, Weiss R, Xu GF, et al.** [A major segment of the neurofibromatosis type 1 gene: cDNA sequence, genomic structure, and point mutations]. Cell. 1990; (62): 193–201.
8. **Chaglassian JH, Riseborough EJ, Hall JE.** [Neurofibromatous scoliosis. Natural history and results of treatment in thirty-seven cases]. J. Bone Joint Surg. Am. 1976; (58): 695–702.
9. **Cnossen MH, de Goede-Bolder A, van den Broek KM, et al.** [A prospective 10 year follow up study of patients with neurofibromatosis type 1] Arch. Dis. Child. 1998; (78): 408–412.
10. **Crawford AH.** [Neurofibromatosis]. In: The pediatric spine: principles and practice, 2nd edition. S.L. Weinstein (ed.). Philadelphia. 2001. P. 471–490.
11. **Crawford AH.** [Neurofibromatosis] // In: The pediatric spine: principles and practice. S.L Weinstein (ed.). N. Y., 1994. P. 619–649.
12. **Durrani AA, Crawford AH, Chouhdry SN, et al.** [Modulation of spinal deformities in patients with neurofibromatosis type 1]. Spine. 2000; (25): 69–75.
13. **Flood BM, Butt WP, Dickson RA.** [Rib penetration of the intervertebral foraminae in neurofibromatosis]. Spine. 1986; (11): 172–174.
14. **Funasaki H, Winter RB, Lonstein JB, et al.** [Pathophysiology of spinal deformities in neurofibromatosis. An analysis of seventy-one patients who had curves associated with dystrophic changes]. J. Bone Joint Surg. Am. 1994; (76): 692–700.
15. **Goldberg NS, Collins FS.** [The hunt for the neurofibromatosis gene] Arch. Dermatol. 1991; (127): 1705–1707.
16. **Kim HW, Wienstein SL.** [Spine update. The management of scoliosis in neurofibromatosis]. Spine. 1997; (22): 2770–2776.
17. **North K.** [Neurofibromatosis type 1: review of the first 200 patients in an Australian clinic]. J. Child Neurol. 1993; (8): 395–402.
18. **Sirois JL, Drennan JC.** [Dystrophic spinal deformity in neurofibromatosis]. J. Pediatr. Orthop. 1990; (10): 522–526.
19. **Vitale MG, Guha A, Skaggs DL.** [Orthodaedic manifestations of neurofibromatosis in children: an update]. Clin. Orthop. Relat. Res. 2002; (401): 107–118.
20. **Tsirikos AI, Saifuddin A, Noordeen MH.** [Spinal deformity in neurofibromatosis type 1: diagnosis and treatment]. Eur. Spine J. 2005; (14): 427–439.

Corresponding author:
Zaydman Alla Mikhailovna
Novosibirsk Research Institute
of Traumatology and Orthopedics
ul. Frunze, 17, Novosibirsk, 630091 Russia
AZaydman@niito.ru

Received March 13, 2008